

THERMIONIC CATHODE-GRID ASSEMBLY SIMULATIONS FOR RF GUNS

V. Volkov, E. Kenjebulatov, S. Krutikhin, G. Kurkin, V. Petrov, E. Rotov, N. Vinokurov,
Budker Institute of Nuclear Physics, Novosibirsk, Russia

Abstract

The projected electron RF gun [1] of the BINP Microtron-Recuperator injector employs a commercial thermionic cathode-grid assembly with 0.08 mm gap, that conventionally used in metal-ceramic RF tubes. Three-dimensional (3D) computer simulations have been performed that use the mesh refinement capability of the both Microwave Studio (MWS) and 2D SAM codes to examine the whole region of the real cathode-grid assembly in static fields in order to illustrate the beam quality that can result from such a gridded structure. These simulations have been found to reproduce the beam current dependency on applied potentials that are observed experimentally. Based on it ASTRA RF beam simulations also predict a complicated time-dependent response to the waveform applied to the grid during the current turn-on, calculation of the dissipated power by electrons at the grid, and particle tracking downstream of the grid into RF gun cavity and further on. These simulations may be representative in other sources, such as some L-band RF injectors for industrial and scientific applications.

INTRODUCTION

The BINP injector was designed to produce a highly space-charge-dominated bunch of about 1.1 nC and 90 MHz repetition frequency. Such an intense beam requires the use of numerical simulation for understanding the propagation characteristics.

The propagation of a beam is sensitive to the details of the initial beam distribution function [2]. In performing simulations of the initial distributions, it is conceptually advantageous to examine the beam starting from the emitter surface.

Such simulations are complex. The RF gun employs a cathode (12 mm diameter) with fine parquet type grid (see Fig.1), having a rectangular cross section wires. Each cell has one narrow wire inside.



Figure 1: Layout of "parquet" type grid.

Such a grid with its 350 cells is well calculated by 3D MWS code assuming static fields. The mesh subdivision was 20 μm . Nevertheless, a calculation by ASTRA tracking code [3] in RF fields requires axially symmetric grid geometry since ASTRA has the unique feature to take into account the aperture in view of a set of cylindrical plugs. So the equivalent axial-symmetric grid has been found for this with help of 2D SAM cod [4].

Instead of a Child-Langmuir model for the cathode emission, as is commonly employed by the both MWS and SAM codes, ASTRA simply emits particles from the cathode surface, with a Gaussian velocity distribution. A thermal spread was assumed to be 0.1 eV. An emitted current exceeds the Child-Langmuir limit, therefore a virtual cathode appears at a distance of 2 μm from the cathode. The thermal emittance of the cathode, according to [5] formulas, is about 1 μm , that is observed by numeric calculations also.

SIMULATION OF THE GRIDDED CATHODE

Each cell of the "parquet" grid (see Fig.1) has overall sizes of 420 \times 840 μm , thickness of 135 μm , and wire width of 60 μm that are 80 μm from the cathode and 0.64 mm distance between grid and anode. The narrow wires have 40 \times 45 μm in cross section. The light transparency is 70 %. The equivalent grid has a set of 27 cylindrical plugs alternated with two cross section sizes similarly to the "parquet" alternation of the normal and narrow wires as shown in Fig.2.

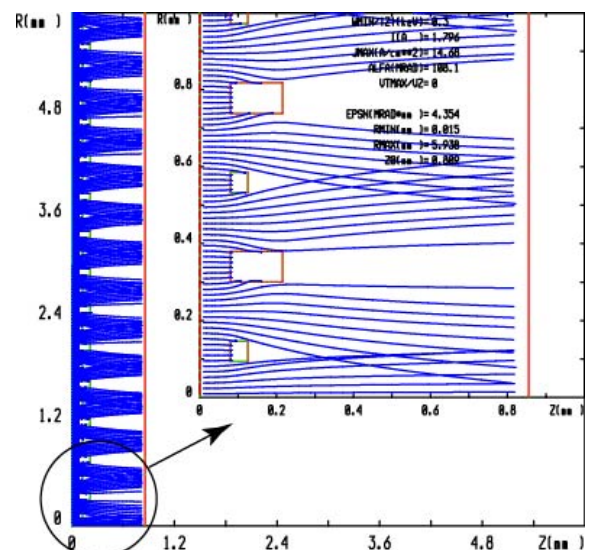


Figure 2: SAM calculations of the equivalent grid.

There are three criteria of the equivalence used: the light transparency is 70 %, static electric field transparencies ($E_{\text{cathode-grid}}/E_{\text{grid-anode}}$) are equal, and emittances in static field are equal for both cases of grids. In such a principle of the equivalency the last condition (emittance equaling) meets automatically with the accuracy of 10% as have been found in numeric calculations.

The numerically calculated behaviors of anode current and grid current versus of grid voltage for the stationary particle flow, observed experimentally, are presented in Figs. 3, 4.

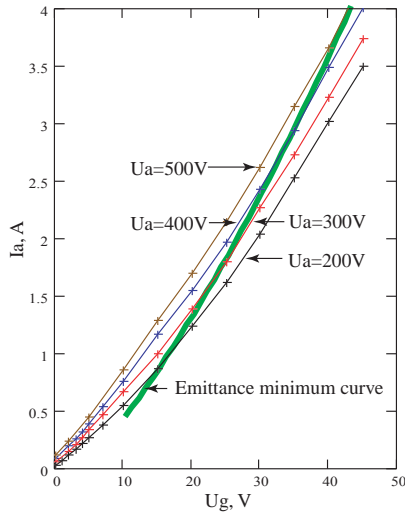


Figure 3: Anode current behaviour vs. grid/anode voltages.

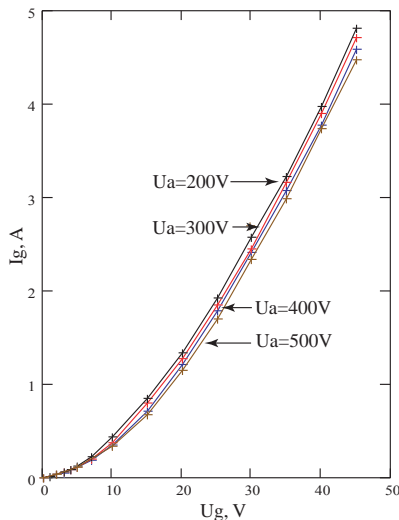


Figure 4: Grid current behaviour vs. grid/anode voltages.

Emittance of a Stationary Particle Flow

When the beam passes through the grid, it is divided into many beamlets. Due to the curved electrical lines around of each grid cell, the beamlets will feel a focusing or defocusing force causing its emittance growth. Theoretically, the emittance growth has a minimum when the electrical fields are equal at both sides of the grid. Our numeric calculations predict this fact; it is presented in Fig. 5. We have to note, as calculations shown, the

absence of narrow wires in each grid cell or all its thickness of 135 μm gives the minimal emittance close to the thermal one (of about 1 μm).

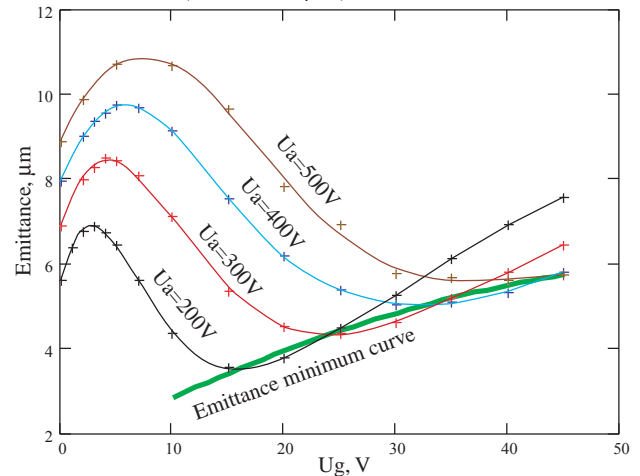


Figure 5: Emittance behaviour versus grid/anode voltages.

FULL RF GUN SIMULATIONS

In these simulations, all calculated static fields of cathode-grid assembly were replaced by RF electric fields whose amplitudes were matched and extended to RF gun fields 90 MHz employed in ASTRA. The temporal behavior of the cathode-grid controlling field (E_{grid}) and RF gun field outside the grid (E_{cavity}) is presented in Fig. 6.

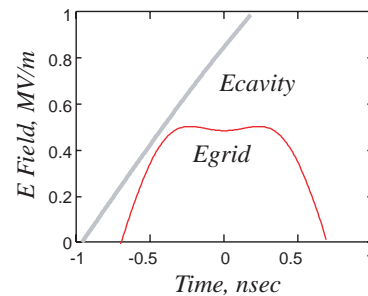


Figure 6: Temporal behaviour of RF gun electric fields.

The substantial numbers of numerical tests have been performed to find the details of this behavior while providing the best beam characteristics, such as the launch 90 MHz phase of 31 degree, the field amplitude strength outside the grid of 2 MV/m and, furthermore, to provide the grid dissipated power by electrons less than 3 W at 90 MHz repetition frequency. These optimized bunch characteristics are presented in Table 1.

Table 1: Optimized bunch characteristics of the RF gun.

Bunch charge, nC	1.23
Normalized r.m.s. bunch emittance, μm	16.2
R.m.s. bunch length, mm	47.2
Average energy of grid captured electrons, eV	18.4
Average grid dissipated power, W	2.96

FULL INJECTOR SIMULATIONS

In the new injector design (see Fig. 7) the bunching cavity is absent, and the beam propagation in RF gun cavity field at 37-degrees off-crest is applied to impart the energy chirp giving sufficient bunch compression in downstream drift space.

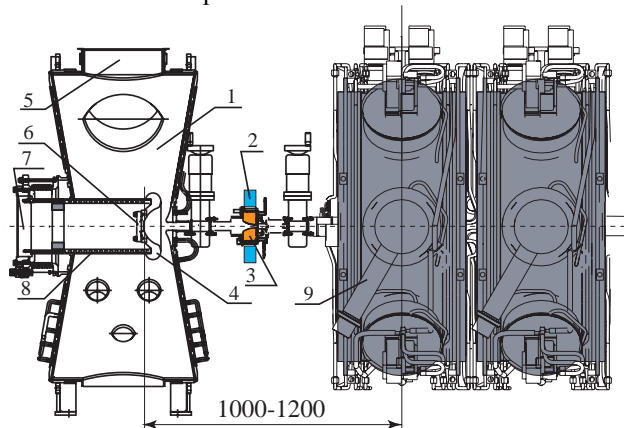


Figure 7: Layout of new BINP injector. 1-RF gun cavity 90 MHz; 2-solenoid; 3-collimator; 4-electrode; 5-RF power input port; 6-cathode-grid assembly flange; 7-tuning mechanism; 8-cavity insertion; 9-accelerating 180 MHz cavities.

The beam emittance depends significantly on the solenoid disposition and its magnetic field. Furthermore, both bunch length and emittance depends on accelerating 180 MHz cavity disposition and its off-crest RF phase. The substantial numbers of numerical tests have been performed to find these optimal values to provide the best beam quality. Two optimized off-crest phases of the RF 180 MHz field of the first accelerating cavity, -30° (increasing field) one for minimal bunch emittance and -60° one for minimal bunch length, have been found.

The emittance and bunch length evolutions while propagating the bunch through the injector is presented in Figs. 8, 9. The optimized bunch characteristics are presented in Table 2.

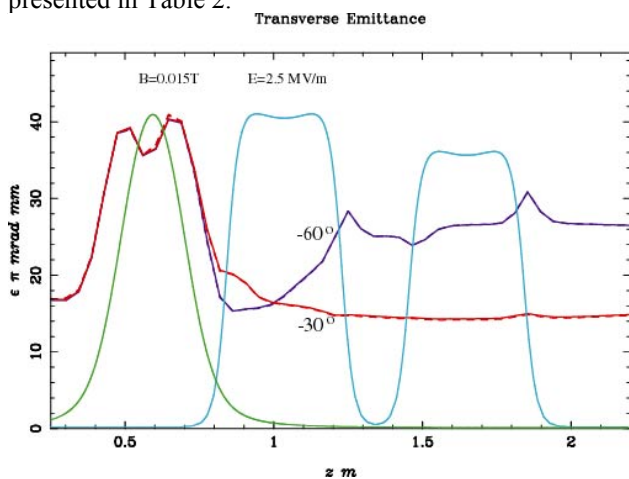


Figure 8: Beam emittance evolution in the BINP injector for optimized off-crest RF phases (-30° and -60°) of the first accelerating 180 MHz cavity.

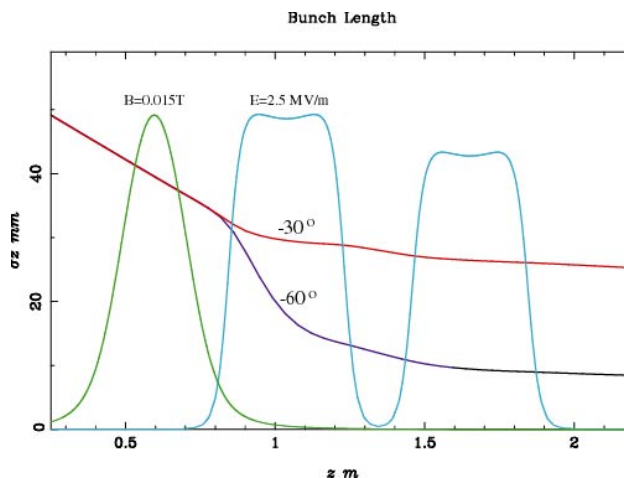


Figure 9: Bunch length evolution in the BINP injector for optimized off-crest RF phases (-30° and -60°) of the first accelerating 180 MHz cavity.

Table 2: Injector-Bunch optimized characteristics

Optimized off-crest RF phase	-30°	-60°
Rms bunch length, mm	25.3	8.4
Normalized r.m.s. emittanc, μm	14.7	26.5
Emittanc of 95% bunch, μm	11	19
Emittanc of 90% bunch, μm	8.7	15.6
R.m.s. energy spread, keV	96	81
Kinetic energy, MeV	1.5	
Repetition frequency, MHz	90	
Average beam current, mA	111	
RF power 90 MHz, kW	≤ 100	
RF power 180 MHz, kW	≤ 300	

ACKNOWLEDGMENTS

The authors thank K. Floettmann for the code ASTRA improvements, and M. Tiunov for the code SAM improvements, both necessary for the grid simulations.

REFERENCES

- [1] V. Volkov, E. Kenjebulatov, S. Krutikhin, G. Kurkin, V. Petrov, I. Sedlyarov, N. Vinokurov. Thermo-Cathode RF Gun for BINP Race-Track Microtron-Recuperator, EPAC08, Genoa, Italy.
- [2] I. Haber et al., PAC05, Knoxville, Tennessee, p2908-2910.
- [3] K. Floettmann, astra User's Manual, http://www.desy.de/~mpyflo/Astra_documentation.
- [4] Ivanov A. V., Tiunov M. A. // Proc. EPAC2002, Paris, 2002, p.1634.
- [5] K. Floettmann, Feb 1997, TESLA-FEL, 97-01.